REQ. NO. 3-9156

CONTRACT REPORT NO. OST83-00198

PERFORMANCE CHARACTERISTICS OF A PROBABILITY SCREENING MACHINE

by

J.M. Beeckmans[1], E. Hu, R. Germain[2]
and A. McIntyre[3]

Submitted to Powder Technology

31 pp

(1) Faculty of Engineering Science
The University of Western Ontario
London, Ontario, Canada

(2) Coal Mining Research Centre
Devon, Alberta, Canada

(3) Crows Nest Resources Ltd.
Calgary, Alberta, Canada

MAR 15 1985
MICROMEDIA

SUMMARY

Data on penetration of particles through single screens in a 0.5 metre wide multiple-deck probability screening machine (Mogensen Sizer), using coal and sand-gravel mixtures, were correlated as a function of the operating variables. The correlations were successfully used to predict the output from the machine with multiple decks in place, both in the laboratory and in a field trial at a coal mine. Misplacement of fines due to adherence to [illegible] particles was found to occur and to depend on the nature of the material and on its moisture content. This factor was not taken into account in the correlations and will lead to very significant errors in some circumstances.

Introduction

A multiple-deck probability screening machine is a device having relatively short and steeply inclined screens, to which vibrations are imparted predominantly in a direction normal to the plane of the screen. Under these conditions the material flows rapidly, and for each screen the cut size (defined as the particle size which has an equal probability of appearing in the underflow and in the overflow to that screen) is substantially smaller than the corresponding aperture size. The principal advantages of probability screening devices are their relatively high throughput rate per unit area, their reduced tendency to blind, and their favourable wear characteristics.

These advantages are to some extent counterbalanced by the fact that probability screens are inherently incapable of a high degree of screening accuracy. On the other hand it should be noted that the screening efficiency of conventional screening machines is never ideal, even at low throughputs, and that it deteriorates with increasing throughput. Furthermore, in many applications a very high level of screening efficiency offers only marginal benefits, in which case a probability screening machine may offer decided advantages over conventional screening machines. It is, however, important to be able to predict the performance of a probability screening machine if a rational decision is to be made concerning its suitability in a particular application, and it was the objective of this study to develop empirical correlations to permit such predictions to be made.

Equipment, Procedures, and Methods for Data Interpretation

The machine used was a 0.5 m. wide Mogensen Sizer (Royer-Mogensen Inc., Kingston, Pa.), a commercial machine which has been used for at least 25 years in Europe, and which has comparatively recently been introduced to North America. Figure 1 shows a schematic of the machine, and Figure 2 illustrates the materials handling facilities used in this study. The feed rate was controlled by the vibrating feeder located at the bottom of the storage silo, and was measured by weighing the material collected in the output drums in a known period of time. The overflow and underflow products were reduced in volume using a sample splitter, and size analyses were performed by sieving, using a Gilson Testing machine for + 1.7 mm material and a Rotap machine for the smaller sizes. The coal used was subbituminous, and came from an Alberta mine.

The range of particle sizes was wide, and the analytical sieve train also covered a wide spectrum of sizes, from 0.212 mm to 12.5 mm. The ratio of aperture sizes of adjacent screens usually equalled $\sqrt{2}$, but in some cases the ratio was 2. In order to extract the maximum information from the data it was thus necessary to interpolate between screen sizes. A number of techniques were investigated, but the following method gave the most consistent results.

A cumulative distribution function, F(x), was calculated for a given

material (either overflow or underflow) from screening analysis data. In order to interpolate between screen sizes x_i and x_{i+1}, a third-order polynomial was fitted to the data in this interval:

$$F(x) = a_0 + a_1x + a_2x^2 + a_3x^3 \qquad (1)$$

The coefficients a_0 - a_3 were calculated by solving four linear equations obtained from four known points on the curve, namely x_{i-1}, $F(x_{i-1})$; x_i, $F(x_i)$; x_{i+1}, $F(x_{i+1})$; and x_{i+2}, $F(x_{i+2})$. (Note that a different set of coefficients must be calculated for each interval.) The function F(x) was not defined over the first and last intervals, since the procedure requires a knowledge of points on the cumulative distribution function beyond the range of each of the individual intervals.

The distribution function f(x) was derived from the cumulative function by differentiation, and was used to calculate the partition function P(x) from the following relation:

$$P(x) = w_o f_o(x)/(w_o f_o(x) + w_u f_u(x)) \qquad (2)$$

P is the partition function, w_o equals the proportion of the feed appearing in the overflow, w_u equals the proportion of the feed appearing in the underflow, $f_o(x)$ equals the distribution function of the overflow, and $f_u(x)$ equals the distribution function of the underflow. The partition function is defined as the proportion of material of size x which reports to the overflow.

The specific penetration function B(x) (Beeckmans and Hill, 1983) is even more fundamental than the partition function. It is defined on the basis that a particle of size x has a probability B(x)dz of penetrating a screen over a differential increment of length dz. Assuming that the specific penetration function remains constant over the length of the screen, the following equation relates B(x) to P(x) for a screen of length L:

$$P(x) = \exp(-B(x)L) \qquad (3)$$

The computed cumulative distribution functions for overflow and underflow were continuous, because each function had to pass through the end points of the respective segments; however discontinuities in slope could and did occur, implying discontinuities in the distribution functions (probability density functions) at the segment boundaries, leading in turn to discontinuities in P(x) and in B(x) at these points. These

discontinuities were generally quite small, and since they are obviously artefacts an additional step was taken to smooth out the curves. This consisted in fitting a fourth-order polynomial by least-squares to the curve of $\ell n(B(x))$ versus x:

$$\ell n(B(x)) = b_0 + b_1 x + b_1 x^2 + b_3 x^3 + b_4 x^4 \qquad (4)$$

The plot of B(x) versus x calculated using equations 1 - 3 was discretized at 50 points, which were then treated as data points for the purpose of least-squares fitting of an equation of the form of Equation 4. Figure 3 is a typical plot of $\ell n(B)$ versus x, showing both the original curve and the smoothed curve.

The smoothed specific penetration curves were then used to calculate five specific diameters, corresponding to partition function values of 0.1, 0.25, 0.5, 0.75 and 0.882. The point with a P-value of 0.5 corresponds to the cut point diameter, that is, to the particle size with equal probability of reporting to the overflow or to the underflow. The P-value of 0.882 corresponds to a B-value of $0.1 m^{-1}$ on a standard 1.25 metre long Mogensen screen. (This size had previously been termed the cutoff diameter (Beeckmans and Hill, 1983)).

The five characteristic diameters were each divided by the correspond-

ing screen aperture, and these ratios were then correlated by multiple linear regression. Feed rate was expressed in the following form:

$$F_r = (F/x_A \rho W)^{0.5} \tag{5}$$

F equals feed rate, W equals screen width, and ρ equals the specific gravity of the material. The square root was found to produce a better fit to the data than the simple argument, and it was therefore used in the regression analyses. Note that feed rate divided by specific gravity is proportional to volumetric feed rate. The presence of the screen aperture size x_A in the denominator is justified on empirical grounds. The independent variables in the regressions were all possible combinations of powers (up to the second-order), and products of the primary variabls F_r, A (vibration amplitude), x_A (screen aperture size), f (vibration frequency), ρ (specific gravity of the feed material) and θ (screen inclination). A hierarchical procedure was used, such that a variable or combination of variables explaining the largest variance was entered first, the variable that explains the greatest amount of variance in conjunction with the first entered next, and so on. In each case the five most significant independent variables, or combinations of variables, were used. This ensured that the resulting expressions were not too cumbersome, and at the same time that no significant factor was excluded. As expected, θ was

found to be a particularly significant variable. Since Mogensen (1965) has shown on theoretical grounds that a critical particle size exists for each given angle, from which it may be inferred that a critical angle exists for each particle size, such that zero penetration occurs, an additional function of θ was included in the regressions to reflect this fact:

$$\eta(\theta) = (42 - \theta)^{-1} \tag{6}$$

The resulting regression equations were as follows:

$$x_{0.10} = [0.994 - 0.00814(f\theta) - 0.00236(A\theta) + 0.0108\ (F_r x_A) - 0.000485\ x_A^2 - 0.0223\ \rho]x_A \tag{7}$$

$$x_{0.25} = [0.945 - 0.00668(f\theta) - 0.562 \times 10^{-5}\theta^3 + 0.00943(F_r x_A) - 0.00204\ (Ax_A) - 0.0250\rho]x_A \tag{8}$$

$$x_{0.50} = [1.074 - 0.00795(f\theta) + 0.00358(F_r x_A) - 0.0312\rho + 0.0169(fF_r) - 1.638\ \eta(\theta)]x_A \tag{9}$$

$$x_{0.75} = [1.2481 - 0.00453(f\theta) + 0.0547(fF_r) - 0.00275(A\theta) - 0.0132\ F_r^2 - 0.0536\ f^2]x_A \quad (10)$$

$$x_{0.882} = [1.322 - 0.00219(f\theta) + 0.0327(fF_r) - 4.36\ \eta(\theta) - 0.0257(fA) - 0.0238\ f^2]x_A \quad (11)$$

The left-hand side of each of these equations gives the predicted particle size corresponding to the value of the ordinate on the partition curve which is indicated by the subscript. On the right-hand side the terms are given in their order of significance in the regression equation. Thus, in each case the product (frequency x angle) explains the largest amount of the observed variance in the data. It is emphasized that all possible combinations of first and second order terms and cross-products were included in the regression, and that only the five most significant terms were retained. Generally speaking the fourth and fifth terms improved the fit to the data only marginally, and little was lost by excluding other terms. Not all of the runs were included in the regression. The first 17 runs were excluded because too few analytical screens were used. Certain other groups were excluded for the same reason, when the critical size-range (P = 0.1 to P = 0.882) was found to have moved into a region which was insufficiently well covered in the analytical sieve

train. A few runs were excluded because for unknown reasons they gave results which were seriously incompatible with the rest of the data. Table 1 gives a summary of some of the parameters of the regression analyses. The ranges of the variables were: frequency: 0.9 - 1.8 kilocycles per minute; amplitude: 3 - 4 mm; feed rate: 0 - 25 tonnes/hr; x_A: 0.85 - 9.5 mm; θ: 18 - 34 degrees. These units must be employed in using equations 7 - 11, since they are not dimensionally homogeneous.

Misplaced Fines and Attrition

In all runs the slope of the partition curve increased with decreasing particle size in the lowest range of sizes, implying that the overflow product contained misplaced fine particles. The anomalous tail region on the partition curve was excluded from the data analysis described by the preceeding section. Several possible mechanisms are suggested for misplacement of fines. These are entrainment of detached fine particles by the motion of large masses of oversize material; entrainment of fine particles attached to the surface of larger particles; creation of fines during the analytical screening process; and creation of fines by attrition during passage through the Mogensen machine.

Inspection of the data showed that misplaced fines were more abundant with coal than with sand or gravel, which suggests that attrition

was a contributing factor. In order to determine if degradation occurred during the analytical screening, a 362 g sample of coal with a bottom size of 3.35 mm was screened in the Gilson screening machine for three successive 5-minute periods, and the weight of material passing the bottom (3.35 mm) screen was determined at the end of each period. The cumulative amounts of fines (minus 3.35 mm material) produced were 17.9, 29.3 and 38.9 g respectively, which shows conclusively that with coal some degradation took place in the Gilson machine.

Regression analyses were performed using as the dependent variable the proportion of the minus 0.212 mm material appearing in the overflow, and using frequency, feed rate, screen angle, vibration amplitude, material specific gravity and screen aperture size as independent variables. As expected, specific gravity was an important variable, since the coal produced relatively more misplaced fines than the sand. Screen aperture size was the next variable in order of importance, followed by screen angle. Feed rate had an insignificant effect on the proportion of fines misplaced, which suggests that entrainment of fines by bulk flow of the oversize product was not a factor. We are thus left with attrition and with entrainment of small particles which become attached to large particles and thereby report to the overflow.

Since sand and gravel are quite hard it seems most unlikely that much

attrition occurred with this material. Furthermore, it was found that while substantial quantities of minus 0.212 mm particles were misplaced, there was virtually no misplacement of material between 0.212 mm and, say, 1 mm. This suggests that the misplaced minus 0.212 mm particles became attached to large particles by surface forces, which were too weak to cause slightly larger particles to adhere throughout the screening. Finally, it was shown in 4 runs made with a damp sand/gravel feed that the proportion of misplaced material below 0.212 mm was substantially larger than predicted by a regression equation derived using only dry sand/gravel data.

The situation with coal is not as clear-cut; however, it should be pointed out that the residence time of coal particles in the Mogensen machine was probably of the order of one or two seconds, whereas the residence time in the analytical sieve train was of the order of 10 minutes or more. It seems probable, therefore, that a substantial proportion of the misplaced fines with coal are an artefact; they were produced after the material has passed through the Mogensen machine. On the other hand, the results with sand/gravel suggest that some of the misplacement is probably due to attachment of fines to larger particles. This mechanism may play a somewhat more prominent role with coal than with sand/gravel, since coal may be said to be a more sticky material.

Discussion

The purely empirical approach employed is justified because the

situation is too complex to interpret in terms of a theoretical model. Although Mogensen (1965) derived equations for predicting the probability that a particle will penetrate the screen on any single contact or bounce, his model is at best approximate, and furthermore there is no way to predict the number of bounces a particle will make, on average, in traversing a given length of screen. Also, Mogensen's model says nothing concerning the effect of feed rate. Lastly, dimensional analysis is not helpful because different screens have different ratios of wire thickness to aperture size, so that they are not geometrically similar. Geometric similarity is also not maintained when a given screen is tilted.

Inspection of the regression equations shows that in all five equations the product term (frequency x angle) is dominant. The effect of angle is understandable, but the equally strong effect found for frequency in combination with angle was unexpected. It should be noted that at a given amplitude of vibration, increasing the frequency increases the vibration velocity of the wire, and this should cause particles to bounce higher and further upon contact with the wire. The effect should be more pronounced at steeper inclinations, because a non-penetrating particle which bounces away from the screen will travel the further before contacting the screen again the steeper angle of inclination of the screen. The coefficients of the terms involving (frequency x angle) are negative, which means that the probability that a particle of a given size will penetrate the screen decreases as the magnitude of this term increases.

The second or third terms in the regression equations all contained the feed rate function F_r, either in the product (F_r x aperture size) or in the product (F_r x frequency). These terms are positive, indicating that the penetration probability for a given size of particle increases with increasing feed rate. Presumably this comes about because at the higher feed rates the particles tend to form a layer above the screen which inhibits or reduces bouncing amplitude, resulting in more bounces per unit length of screen and hence in increased likelyhood of penetration.

Particle density enters as a variable primarily in connection with the variable F_r (equation 5), but also directly in the regression equations for $x_{0.1}$ and for $x_{0.25}$ (equations 7 and 8). The latter terms are, however, only of marginal significance, and the effect of density is thus minor when feed rate is expressed in terms of volume of material rather than mass of material per unit time.

Extension to the Multi-Deck Situation

A number of runs were performed with multiple screens in place. The correlations developed from single-screen data were used to predict the performance of Mogensen machine using multiple screens, and these predictions were compared with the corresponding experimental data.

Flow through and over screens other than the top screen was calculated by integrating the following set of equations:

For $j = 2$ to $j = k$ (k equals the number of screens)

$$d(\Delta M_j(z, x)) = -\Delta M_j(z, x)B_j(x)dz + \Delta M_{j-1}(z, x)B_{j-1}(x)dz \qquad (12)$$

subject to boundary conditions

$$\begin{aligned} \Delta M_j(0, x) &= 0 \qquad j \neq 1 \\ \Delta M_1(0, x) &= Ff(x)dx \end{aligned} \qquad (13)$$

$\Delta M_j(z,x)$ equals the rate of flow of particles whose size lies in the interval $(x, x + \Delta x)$, above screen j at a distance z from the feed point; $B_j(x)$ is the specific penetration function pertaining to screen j, F equals the feed rate and $f(x)$ is the size distribution function of the feed. The overflow flowrate over screen j is

$$O_j = \int_0^\infty \Delta M_j(L, x)dx \qquad (14)$$

Flow over the top screen was computed by an equation analogous to equation (12), but with the second term on the right of the equal sign deleted.

Equation 12 implies that material penetrating screen j at a distance z along that screen from its leading edge lands on the next screen at a point which is at the same distance z from the beginning of that screen as measured along its surface. This assumption is obviously only approximately true, since the screens are to some extent offset (ie. their leading edges do not lie in a vertical plane) and they are inclined at differing angles, and also because the material which penetrates a screen at a particular point would be expected to land over a finite area of the screen below rather than at a fixed distance from its leading edge. Finally, the flowrate of underflow through the bottom screen is found from the equation

$$U = F - \sum_{j=1}^{k} O_j \qquad (15)$$

A computer program was written which predicts the distribution of particles in the various outlet streams of the Mogensen, using the previous theory. The inputs include a screen analysis of the feed material, the feed rate, and the number, aperture size, angle of inclination, frequency and amplitude of vibration of the screens. For greater computational accuracy the size-intervals between analytical screens (ie. the screens used to express the size-distribution of the feed) were further sub-divided into nine sub-intervals, and the fraction of material at each sub-interval size appearing in each of the outlets was computed. A comparison between

the predictions of the program and experimental data from a typical run is shown in Figure 4. It should be pointed out that the deviations between prediction and experiment with small particles for the overflow to the first two screens are due to entrainment of fines. With the exception of this region, the agreement is quite good. Agreement between theory and experiment was similar with the other multi-screen data obtained.

Data obtained in tests at a coal mine (Crows Nest Resources Ltd.'s mine at Line Creek, British Columbia) with a 0.5 m wide Mogensen Sizer were also compared with predictions of the program. The Mogensen application being considered involves splitting the underflow from an existing 9 mm screen at approximately 2 mm, and treating the +2 mm material in a heavy media cyclone. The overflows from the top four screens were combined to yield an overflow product. Screen sizes were 9.5, 5.7, 4.0, 3.4 and 2.8 mm inclined at the usual angles (18, 24, 30, 32.5 and 34 degrees). Predicted and observed size distributions are shown plotted in Figures 5 and 6, for coals containing 4.7% and 8.7% moisture respectively. Agreement between theory and experiment is clearly better with the lower moisture content coal, as expected. However, even with the lowest moisture coal there is a significant amount of carry-over of fines with the overflow due to adherence to larger particles. As indicated earlier, misplacement of fines was also observed in the tests performed with sand and air-dried coal at the Coal Mining Research Centre; however its extent in that case was considerably smaller. Finally, it is noted that with the higher-moisture

coal (8.7%) fines became attached to the screens, in some cases to the point of choking them. This phenomenon is to be distinguished from blinding, which is caused by the lodging of particles which are slightly larger than the screen aperture. Choking of a screen by wet fines would clearly have a very detrimental effect on screen performance.

Summary and Conclusions

Experimental data on screening of coal and of sand/gravel mixtures, obtained with a 0.5 metre wide Mogensen Sizer, were used to correlate certain characteristic points on the specific penetration curve against the following independent variables: feed rate, angle of inclination of the screen, screen aperture size, vibration frequency and amplitude, and material specific gravity. The correlations were also used in conjunction with some basic theory, to predict the performance of the Mogensen sizer with several screens in place. These predictions agreed quite well with experimental data for low moisture feeds, except for the finest particle region, where significant attachment of small particles to large particles probably occurred. The model of the Mogensen Sizer developed in conjunction with this project has been added to the Canada Department of Energy, Mines and Resources' SPOC simulation system library of computer programs, and may be accessed directly.

Literature Cited

Beeckmans, J.M. and Hill, J. (1983). Powder Technol. 35, 263.

Mogensen, F.K. (1965). Quarry Manager's J., October issue, 409.

Acknowledgements

The authors wish to express their appreciation to Crows Nest Resources Ltd. for financial support which made this study possible.

NOMENCLATURE

A	Amplitude of vibration (mm)
a_0, a_1	Polynomial coefficients (equation 1)
b_0, b_1	Polynomial coefficients (equation 4)
$B_j(x)$	Specific penetration function for j'th screen (m^{-1})
F	Feed rate function (tonnes hr^{-1})
F_r	Feed rate function (equation 5) (tonnes$^{1/2}$ $m^{-1/2}$ $hr^{-1/2}$ $mm^{-1/2}$)
f	Frequency (kilocycles per minute)
$f(x)$	Size distribution function of the feed (mm^{-1})
$f_o(x)$	Size distribution function of the overflow (mm^{-1})
$f_u(x)$	Size distribution function of the underflow (mm^{-1})
k	Number of screens
L	Screen length (m)
$\Delta M_j(z,x)$	Rate of flow of particles, whose size lies in the interval x to Δx, on screen j at a distance x from the origin (tonnes hr^{-1})

O_j	Overflow flow rate of j'th screen (tonnes hr^{-1})
$P(x)$	Partition function (-)
U	Underflow flow rate (tonnes hr^{-1})
W	Screen width (m)
w_o	Proportion of the feed recovered in the overflow (-)
w_u	Proportion of the feed recovered in the underflow (-)
x	Particle size (mm)
x_A	Screen aperture size (mm)
x_r	Size predicted by the regression to correspond to value p for P(x) (mm)
z	Distance along the screen from the feed point (m)

GREEK SYMBOLS

ρ	Specific gravity (-)
$\eta(\theta)$	Empirical function (equation 6) (-)
θ	Angle of inclination of the screen (degrees)

Table 1

Parameters Pertaining to Regression Analyses

Dependent Variable	Number of runs	Standard Deviation	r^2
$x_{0.1}/x_A$	163	0.052	0.84
$x_{0.25}/x_A$	165	0.052	0.82
$x_{0.5}/x_A$	165	0.041	0.84
$x_{0.75}/x_A$	165	0.045	0.78
$x_{0.882}/x_A$	165	0.046	0.78

Captions for Figures

Figure 1 Vertical section through the Mogensen Sizer. I: feed port; V: vibrators; O: outlet ports; B: internal baffles. (Note: baffles may be inserted to yield from 2 to 6 products. Two products only are produced from the arrangement shown in this sketch.)

Figure 2 Schematic of the equipment layout. 1 silo; 2 feeders; 3 bucket elevator; 4 Mogensen Sizer; 5 overflow outlets; 6 underflow outlets.

Figure 3 Typical plot of penetration function versus particle size. ($\theta = 18°$, $x_A = 2.36$ mm, F/W = 2.56 tonnes $m^{-1}hr^{-1}$, f = 1.8 kilocycles/min, A = 3 mm). Solid curve: plot as calculated initially; stippled curve: curve after smoothing (equation 4).

Figure 4 Cumulative distribution functions obtained with multiple screens. O_1, O_2, O_3: overflows to screens 1, 2, 3; U: underflow to screen 3. Points are experimental data, lines are predicted curves. ($\theta_1 = 18°$, $\theta_2 = 24°$, $\theta_3 = 30°$, $x_{A1} = 9.5$ mm, $x_{A2} = 4.75$mm $x_{A3} = 0.85$ mm, F = 44.2 tonnes $m^{-1}hr^{-1}$, f = 1.8 kilocycles/min, A = 3mm).

Figure 5 Experimental (points) and predicted (curves) cumulative distribution functions of underflow and overflow products from run-of-mine coal (moisture content 4.7%). Overflows from four screens combined to yield overflow product.

Figure 6 Experimental (points) and predicted (curves) cumulative distribution functions of underflow and overflow products from run-of-mine coal (moisture content 8.7%). Overflows from five screen combined to yield overflow product.

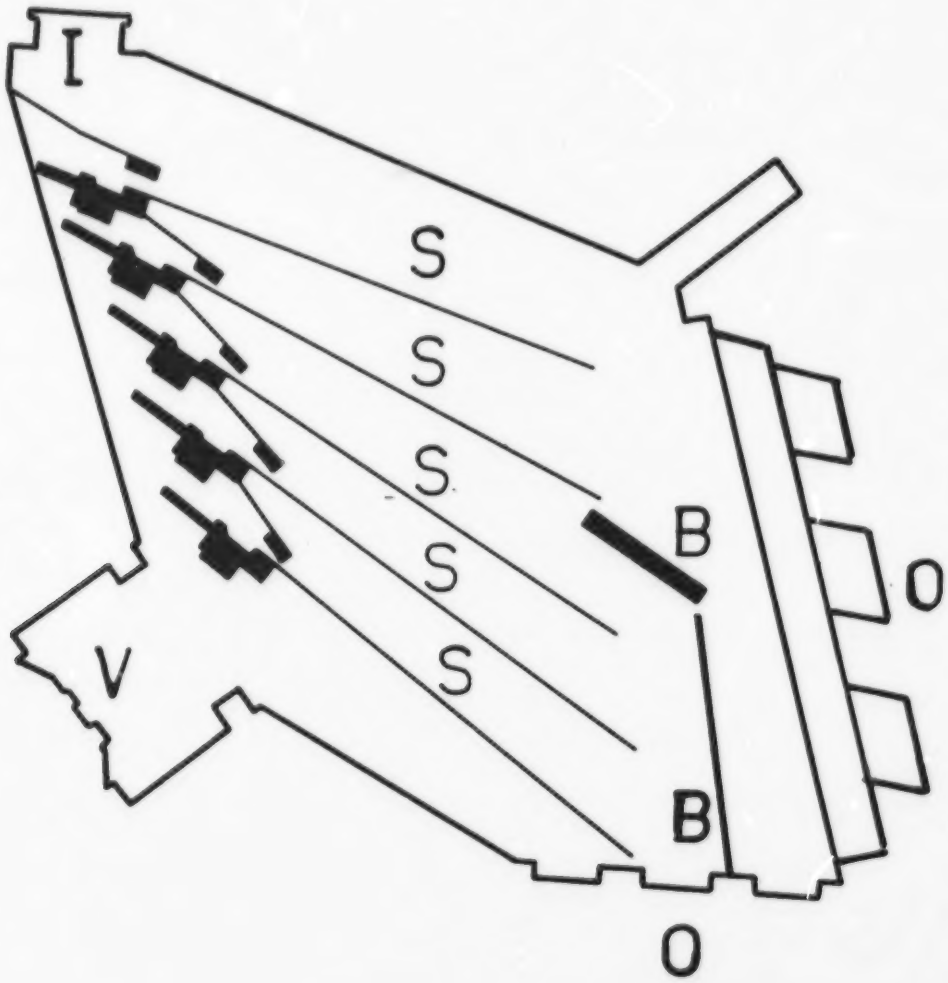

Figure 1

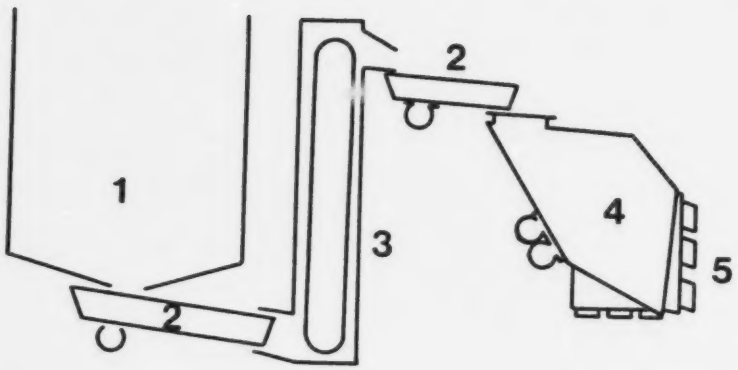

Figure 2

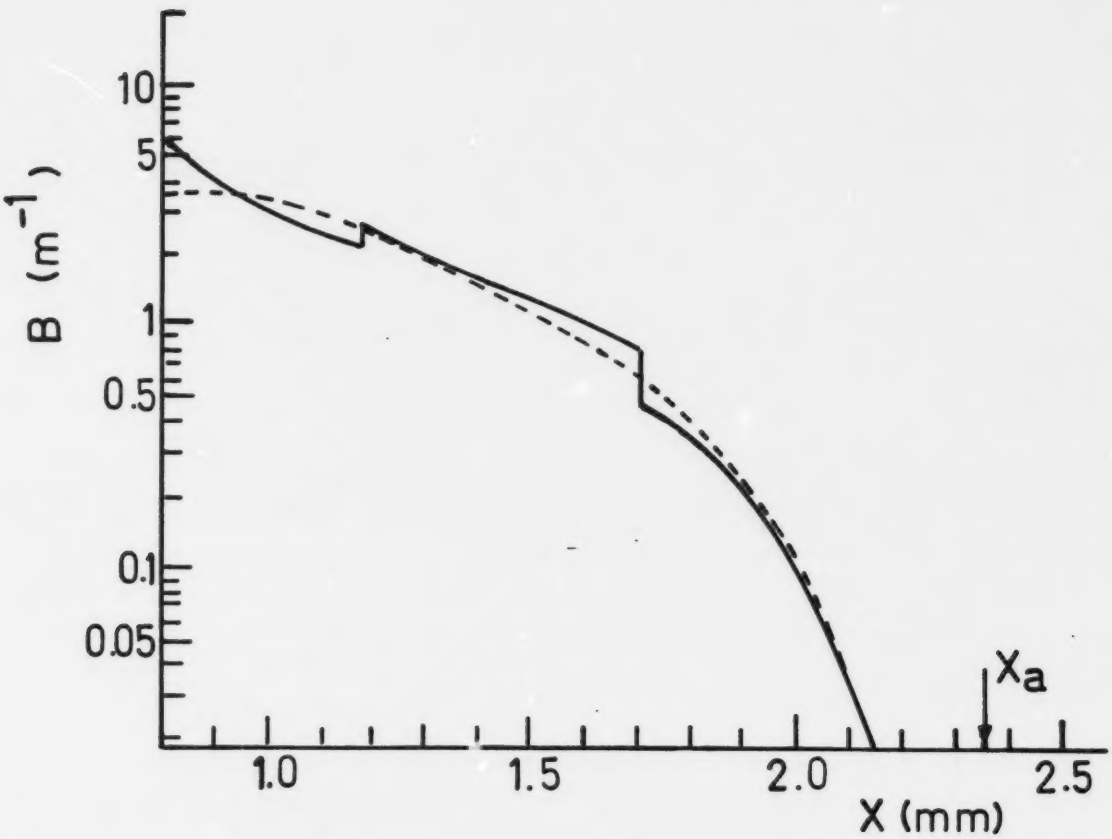

Figure 3

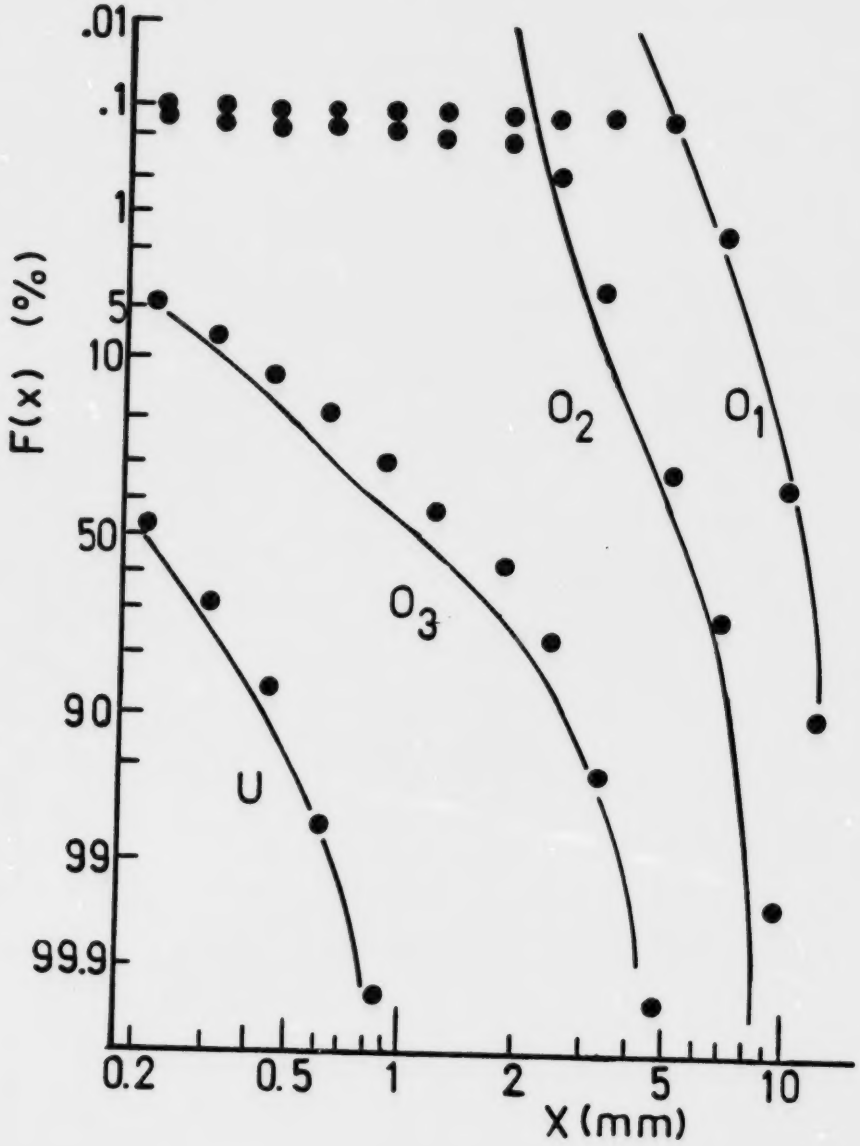

Figure 4

Figure 5

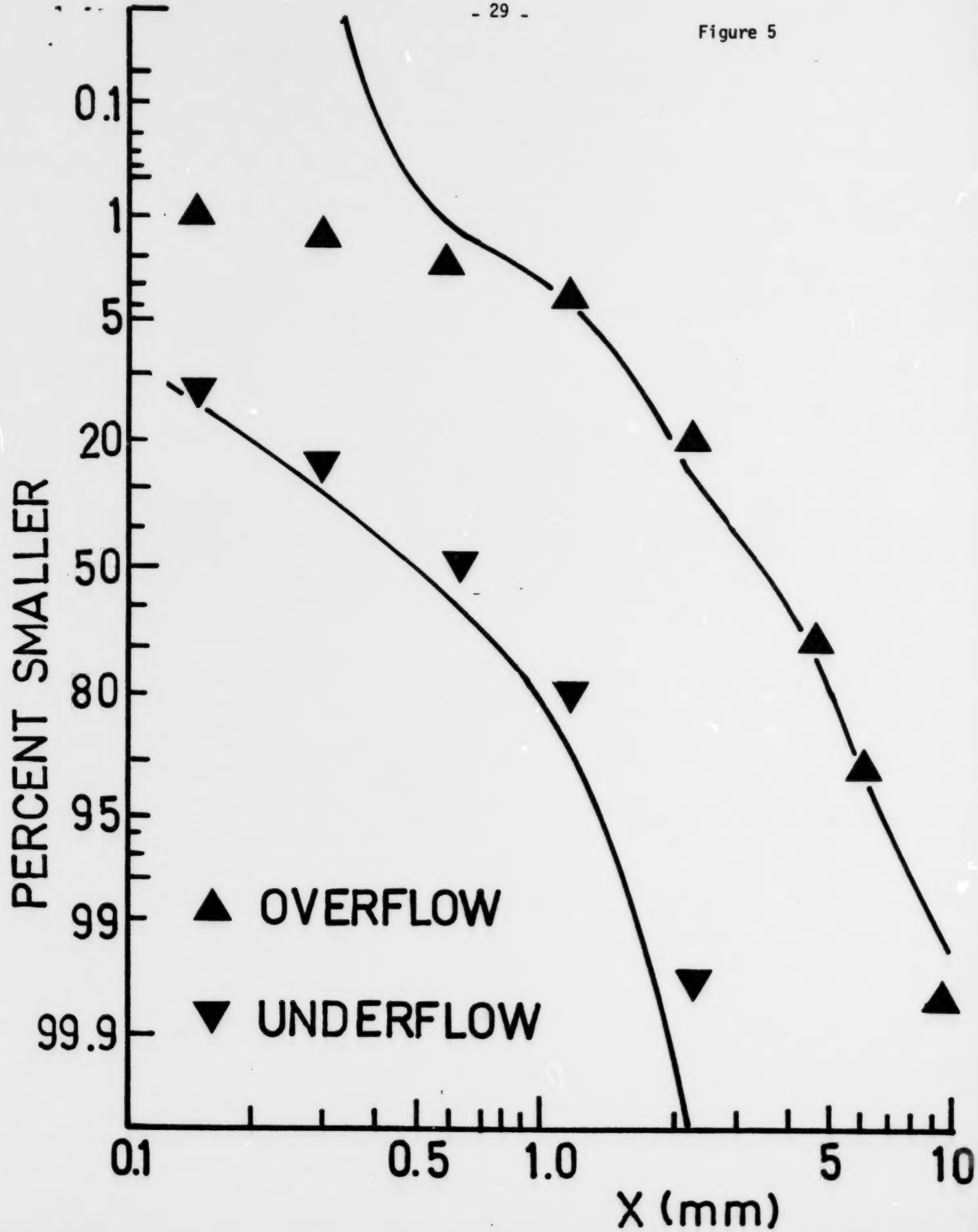
PERCENT SMALLER
0.1
1
5
20
50
80
95
99
99.9
▲ OVERFLOW
▼ UNDERFLOW
0.1
0.5
1.0
5
10
X (mm)

Figure 6

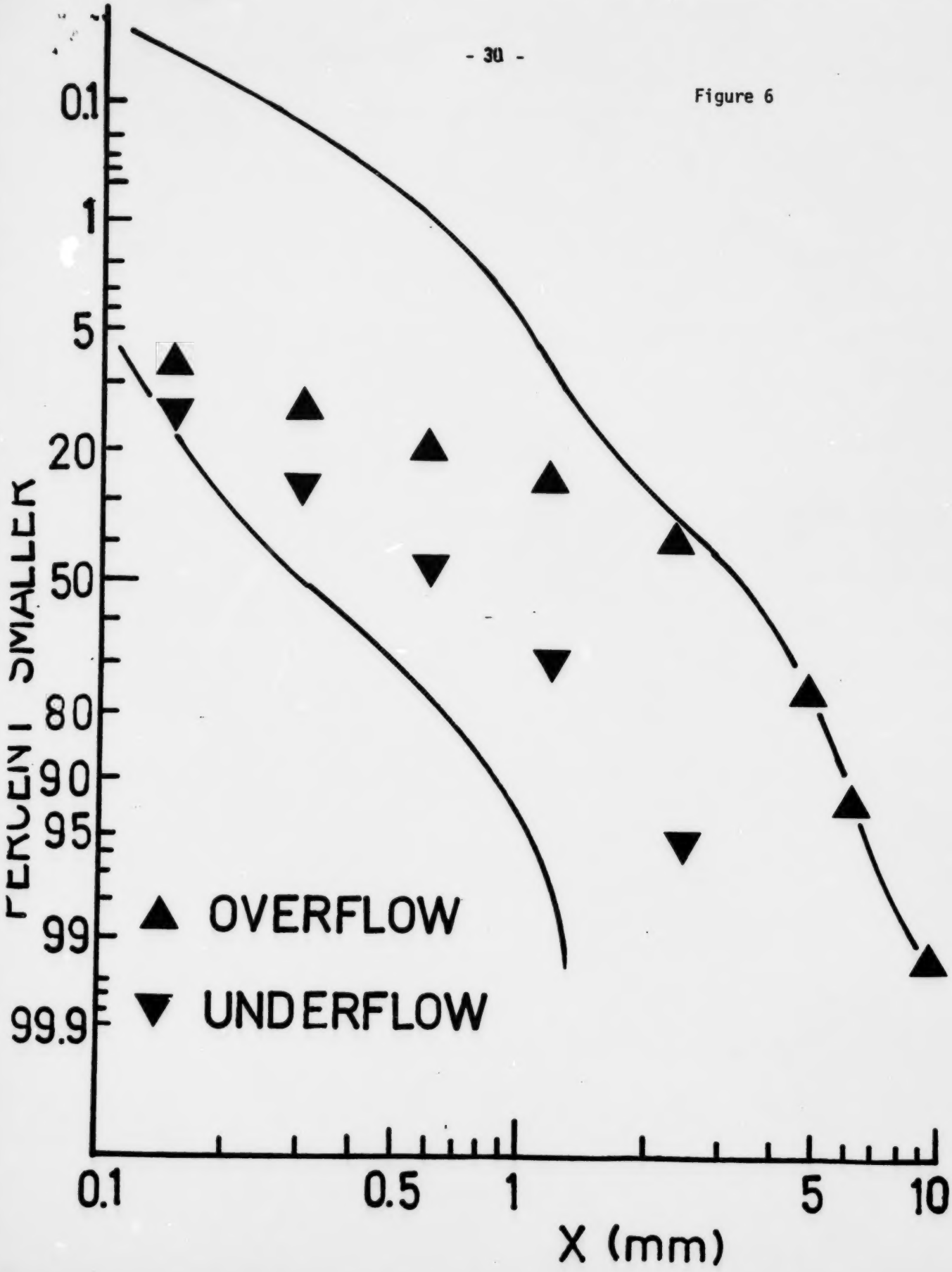
0.1
1
5
20
50
80
90
95
99
99.9
PERCENT SMALLER
OVERFLOW
UNDERFLOW
0.1
0.5
1
5
10
X (mm)